J. Fluid Mech. (1973), *vol.* 59, *part* 1, *pp.* 187–206
Printed in Great Britain

Bubble transport theory with application to the upper ocean

By G. A. GARRETTSON

Physics Department, Naval Postgraduate School, Monterey, California

(Received 19 June 1972 and in revised form 3 January 1973)

The formalism of transport theory is adapted to a general description of bubble populations in a moving fluid. The bubble distribution, as a function of position, velocity, radius and time, satisfies a Boltzmann-type transport equation that is derived and then formally solved by the method of characteristics. In order to apply this new analytical tool to the specific problem of gas bubble transport in the upper ocean, an ocean model and a bubble dynamics model must be chosen. For the purpose of illustration, explicit solutions are written for distributed sources in a stationary ocean with simple expressions for bubble gas diffusion and drag. Calculated results clarify the relations between observed bubble distributions at sea, proposed bubble source mechanisms and known models of single-bubble dynamics.

1. Introduction

The solutions of many experimental and engineering problems depend upon a knowledge of bubble distributions in a fluid medium. For instance, gas bubbles near the surface of the ocean are important in a variety of subjects that include underwater sound propagation (Shulkin 1968, 1969), meteorology (Blanchard & Woodcock 1957), sea surface chemistry (Sutcliffe, Baylor & Menzel 1963), cavitation (Fox & Herzfeld 1954) and air–sea gas exchange (Kanwisher 1963). Several efforts have been made to measure bubble densities in the ocean (Blanchard & Woodcock 1957; Glotov, Kolobaev & Neuimin 1962; McCartney & Bary 1965), the most recent being that by Medwin (1970). To infer near-surface bubble populations from *in situ* measurements of acoustic attenuation, Medwin exploited the fact that a gas bubble's scattering and absorption cross-sections for sound at the bubble resonant frequency can typically be 1000 times its geometrical cross-section. For this reason large bubble densities near the sea surface can significantly affect underwater sound transmission.

Many complex factors affect bubble distributions in a fluid such as the ocean, and some of these phenomena have been carefully investigated. For example, LeBlond (1969*a*, *b*) examined gas diffusion from an ascending bubble, and Levich (1962, chap 8) is an excellent reference on single-bubble dynamics. The purpose of this paper is to develop and to demonstrate new analytical tools for investigating relationships between observed bubble distributions and the phenomena which create, transport and eliminate bubbles.

In §§ 2 and 3 the formalism of transport theory is adapted to the general problem

of describing bubble populations in a moving fluid. The bubble distribution, as a function of position, time, velocity and radius, satisfies a Boltzmann-type transport equation that is derived. Using a Lagrangian viewpoint, the formal solution is expressed as a line integral of the volume source function along characteristic curves. In § 4 general expressions are obtained for bubble acceleration and radius change rate and some known models of gas diffusion and bubble drag are introduced. Finally, in the context of gas bubble transport in the upper ocean, a simple model is chosen to illustrate the utility of transport theory. Calculated results clarify relationships between observed bubble distributions, proposed bubble source mechanisms and known models of single-bubble dynamics.

2. The bubble transport equation

Consider the problem of describing the bubble distribution, as a function of position $\mathbf{r}$, velocity $\mathbf{v}$, size l and time t, in a moving fluid that may contain bubble sources and sinks. In general, a 'bubble' might be considered as any simple, closed region containing a fluid somehow different from the transporting medium. Since examples chosen in this paper refer primarily to spherical gas bubbles, l will represent the bubble radius. However, if the bubbles are not spherical, then l might represent the radius of a spherical volume equal to the actual bubble volume, or one might wish to generalize the description to include more than one parameter for size.

Suppose that the time evolution of the position, the velocity and the radius of each bubble depends only upon the properties of the medium and the bubble characteristics and is statistically independent of the state of any other bubble. Then define the bubble distribution function $\psi(\mathbf{r}, \mathbf{v}, l, t)\, d^3r\, d^3v\, dl$ as the mean number of bubbles at time t in the volume d^3r about $\mathbf{r}$ with velocity in d^3v about $\mathbf{v}$ and radius in dl about l.† Furthermore, if bubbles interact with one another, suppose that no more than two interact at any one time and that the collision time is short compared with the time required for ψ to change appreciably. Then ψ satisfies a Boltzmann-type transport equation whose solution describes the ensemble-average behaviour of the bubble population in terms of single-bubble behaviour.

At this point it is convenient to define the seven-dimensional volume element $d^7\tau \equiv d^3r\, d^3v\, dl$ and to adopt a Lagrangian viewpoint. In the time interval $(t, t+dt)$ the bubbles that were in $d^7\tau$ about $(\mathbf{r}, \mathbf{v}, l)$ have moved to a new volume $d^7\tau$ about $(\mathbf{r}', \mathbf{v}', l')$, where the primed quantities refer to the time $t+dt$ and the unprimed quantities refer to the time t. This transport occurs through a change in position due to a velocity $\mathbf{v} \equiv d\mathbf{r}/dt$, through a change in velocity due to an acceleration $\mathbf{a} \equiv d\mathbf{v}/dt$, and through a change in radius due to a radius rate of change $\nu \equiv dl/dt$:

$$\left.\begin{aligned} \mathbf{r}' &= \mathbf{r} + \mathbf{v}\,dt + O(dt^2), \\ \mathbf{v}' &= \mathbf{v} + \mathbf{a}\,dt + O(dt^2), \\ l' &= l + \nu\,dt + O(dt^2) \end{aligned}\right\} \tag{1}$$

† For example, in the Cartesian representation, position components lie in the intervals $(x, x+dx)$, $(y, y+dy)$ and $(z, z+dz)$; velocity components lie in the intervals (v_x, v_x+dv_x), (v_y, v_y+dv_y) and (v_z, v_z+dv_z); and the radius is in the interval $(l, l+dl)$.

(Taylor series about time t). For gas bubbles in the ocean and elsewhere, the acceleration results from several influences that include gravity, buoyancy and entrainment of bubbles by the fluid, while the rate of change of bubble radii is caused by hydrodynamic compression, surface tension and gas diffusion. Expressions for $\mathbf{a}$ and ν are obtained in §4, where single-bubble dynamics is discussed.

Conservation of bubbles demands that the number $\psi(\mathbf{r}', \mathbf{v}', l', t+dt)\, d^7\tau'$ of bubbles in the volume element at time $t+dt$ be equal to the number

$$\psi(\mathbf{r}, \mathbf{v}, l, t)\, d^7\tau$$

that start in the volume element at time t, plus (minus) any bubbles that are introduced (lost) by distributed sources (sinks), $S(\mathbf{r}, \mathbf{v}, l, t)\, d^7\tau\, dt$:

$$\psi(\mathbf{r}', \mathbf{v}', l', t+dt)\, d^7\tau' - \psi(\mathbf{r}, \mathbf{v}, l, t)\, d^7\tau = S(\mathbf{r}, \mathbf{v}, l, t)\, d^7\tau\, dt + O(dt^2), \tag{2}$$

where $S(\mathbf{r}, \mathbf{v}, l, t)\, d^7\tau$ is the rate at which bubbles are introduced into $d^7\tau$ about $(\mathbf{r}, \mathbf{v}, l)$ by distributed sources. To develop (2) it is sufficient to note that terms of $O(dt^2)$ will disappear in the limit $dt \to 0$. Therefore we expand

$$\psi' \equiv \psi(\mathbf{r}', \mathbf{v}', l', t+dt)$$

in a Taylor series about $\psi \equiv \psi(\mathbf{r}, \mathbf{v}, l, t)$ and keep terms of order up to dt:

$$\psi' = \psi + (\partial\psi/\partial t)\, dt + (\mathbf{v} \cdot \nabla_r \psi)\, dt + (\mathbf{a} \cdot \nabla_v \psi)\, dt + \nu(\partial\psi/\partial l)\, dt + O(dt^2), \tag{3}$$

where

$$\nabla_r(\ ) \equiv (\partial(\ )/\partial x, \partial(\ )/\partial y, \partial(\ )/z) \quad \text{and} \quad \nabla_v(\ ) \equiv (\partial(\ )/\partial v_x, \partial(\ )/\partial v_y, \partial(\ )/\partial v_z)$$

are Cartesian representations of the gradient operators in position space and velocity space, respectively.

To proceed, $d^7\tau'$ must be expressed in terms of $d^7\tau$:

$$d^7\tau' = \gamma(t+dt, t)\, d^7\tau, \tag{4}$$

where

$$\gamma(t+dt, t) \equiv \partial(\mathbf{r}', \mathbf{v}', l')/\partial(\mathbf{r}, \mathbf{v}, l) \tag{5}$$

$$= 1 + (\nabla_v \cdot \mathbf{a})\, dt + (\partial\nu/\partial l)\, dt + O(dt^2) \tag{6}$$

is the Jacobian that is obtained by using (1) in (5). Substituting (3), (4) and (6) into (2), collecting terms of $O(dt)$, dividing by $d^7\tau\, dt$ and taking the limit $dt \to 0$ yields the *bubble transport equation*:

$$\partial\psi/\partial t + \mathbf{v} \cdot \nabla_r \psi + \mathbf{a} \cdot \nabla_v \psi + \nu\, \partial\psi/\partial l = S - \Sigma_t \psi, \tag{7}$$

where

$$\Sigma_t \equiv \nabla_v \cdot \mathbf{a} + \partial\nu/\partial l \tag{8}$$

and where $-\infty < x, y, z < \infty$, $-\infty < v_x, v_y, v_z < \infty$ and $0 < l < \infty$.

A simpler (but less rigorous) derivation of (7) is obtained by recognizing that $\mathbf{v}\psi$, $\mathbf{a}\psi$ and $\nu\psi$ are the fluxes of bubbles in position space, velocity space and radius space, respectively. Then

$$\mathscr{F} \equiv -\{\nabla_r \cdot (\mathbf{v}\psi) + \nabla_v(\mathbf{a}\psi) + \partial(\nu\psi)/\partial l\}$$

is the net flux of bubbles into $d^7\tau$ by virtue of 'streaming' in seven-dimensional space $(\mathbf{r}, \mathbf{v}, l)$. Since the time rate of change of ψ in $d^7\tau$ is due to bubble streaming

into $d^7\tau$, as well as to other sources S, we have $\partial\psi/\partial t = \mathscr{F} + S$. Using the identity $\nabla_v.(a\psi) = \mathbf{a}.\nabla_v\psi + \psi\nabla_v.\mathbf{a}$ and the fact that $\mathbf{r}$ and $\mathbf{v}$ are independent variables $(\nabla_r.\mathbf{v} = 0)$ yields (7).

The term $\Sigma_t\psi$ in the bubble transport equation is generally non-zero owing to the functional dependence of acceleration $\mathbf{a}(\mathbf{r}, \mathbf{v}, l, t)$ and radius change rate $\nu(\mathbf{r}, \mathbf{v}, l, t)$ on the bubble velocity and radius, respectively. This is unusual since in transport equations normally encountered, the term corresponding to $\Sigma_t\psi$ is generally zero (Chapman & Cowling 1964, pp. 46, 322). Mathematically, $\Sigma_t \neq 0$ causes the volume element

$$d^7\tau' = [1 + \Sigma_t dt + O(dt^2)]\, d^7\tau$$

to change appreciably in the time interval dt. Physically, the term $-\Sigma_t\psi$ on the right-hand side of (7) acts as a pseudo-source, or sink, depending upon the functional form of $\mathbf{a}$ and ν.

For example, suppose that $\mathbf{a}$ is proportional to $-\mathbf{v}$. Then $\nabla_v.\mathbf{a} < 0$, and the bubbles are decelerated into a smaller volume $d^3v' = (1 + \nabla_v.\mathbf{a}\, dt)\, d^3v$. This increases the density so $-(\nabla_v.\mathbf{a})\,\psi$ acts like a 'source' in (7). Similarly, suppose that ν is proportional to $v_z l$, so that $\partial\nu/\partial l$ is proportional to v_z. For $v_z > 0$ the bubble radii are increasing and becoming more spread out over a larger interval $dl' = (1 + (\partial\nu/\partial l)\, dt)\, dl$. This decreases the density, so $-(\partial\nu/\partial l)\,\psi$ acts like a 'sink' in (7).

The second term on the right-hand side of (7), $S(\mathbf{r}, \mathbf{v}, l, t)$, represents distributed bubble sources and sinks. In addition to external sources and sinks, this term can include the effects of phenomena such as bubble scattering off small-scale turbulent eddies, bubble–bubble interactions, etc. For instance, when the scale of turbulent eddies is of the order of the bubble radius, they will be referred to as 'small scale', and bubbles entrained by the fluid may scatter off them. To handle this phenomenon one could define a turbulent scattering cross-section Σ_s such that

$$\Sigma_s(\mathbf{r}, \mathbf{v}_1 \to \mathbf{v}, l_1 \to l, t)\, v_1\psi(\mathbf{r}, \mathbf{v}_1, l_1, t)\, d^3v_1\, dl_1\, d^7\tau$$

represents the probable rate at which bubbles in d^3r about $\mathbf{r}$ at time t are scattered by turbulent eddies from d^3v_1 about $\mathbf{v}_1$ and dl_1 about l_1 into d^3v about v and dl about l, where $v_1 = |\mathbf{v}_1|$ is the speed. Then

$$S(\mathbf{r}, \mathbf{v}, l, t) = \int \Sigma_s(\mathbf{r}, \mathbf{v}_1 \to \mathbf{v}, l_1 \to l, t)\, v_1\psi(\mathbf{r}, \mathbf{v}_1, l_1, t)\, d^3v_1\, dl_1 - v\psi(\mathbf{r}, \mathbf{v}, l, t) \int \Sigma_s(\mathbf{r}, \mathbf{v} \to \mathbf{v}_1, l \to l_1, t)\, d^3v_1\, dl_1 \qquad (9)$$

represents the net rate at which bubbles are introduced into $d^7\tau$. Specification of Σ_s requires detailed knowledge of the turbulent field as well as a model for bubble–eddy interaction.

Substitution of (9) into (7) results in an integro-differential bubble transport equation. If bubble–bubble interactions are included, the bubble transport equation is nonlinear as well (Chapman & Cowling 1964, p. 63). Below the surface in the upper ocean the average separation between bubbles is about 1000 times the bubble radii (Medwin 1970), but very near or at the surface wave action can

cause higher bubble densities. In addition, the energy contained in small-scale turbulence appears to increase with wave action but to decrease with depth (Shonting 1968). To avoid at this time obvious analytical complications, the bubble density will be assumed low enough so that bubble–bubble interactions are negligible. It will also be assumed that the energy contained in small-scale turbulence is negligibly small, so that the bubbles are partially entrained by the fluid without abrupt changes in velocity or radius. In the ocean these assumptions should be valid except very near the surface during heavy seas.

Suppose that the source $S(\mathbf{r}, \mathbf{v}, l, t)$ is independent of ψ or, at most, is proportional to ψ:

$$S = S_1 + \Sigma_1 \psi. \tag{10}$$

This mathematical simplification yields a linear, first-order, partial differential bubble transport equation whose formal solution is outlined in the next section. It is worthwhile to note that the simplifying assumption (10) is not a severe limitation for many problems involving gas bubble transport in the upper ocean. All external bubble sources such as surface waves, rain and snow nucleation, organic decay and photosynthesis can be included, as well as simple models of bubble scattering, absorption and creation that have the form (10).

3. Solution by method of characteristics

The first-order partial differential equation (7) is equivalent to the following set of eight simultaneous, first-order ordinary differential equations with initial conditions:

$$d\mathbf{r}/dt = \mathbf{v}, \quad -\infty < x, y, z < \infty; \qquad \mathbf{r}(t_0) = \mathbf{r}_0 = (x_0, y_0, z_0); \tag{11a–c}$$

$$d\mathbf{v}/dt = \mathbf{a}, \quad -\infty < v_x, v_y, v_z < \infty; \qquad \mathbf{v}(t_0) = \mathbf{v}_0 = (v_{x0}, v_{y0}, v_{z0}); \tag{11d–f}$$

$$dl/dt = \nu, \quad 0 \leqslant l < \infty; \qquad l(t_0) = l_0; \tag{11g}$$

$$d\psi/dt = S - \Sigma_t \psi, \quad 0 \leqslant \psi < \infty; \qquad \psi(t_0) = \psi_0. \tag{12}$$

The equivalence of these 'characteristic equations' and the bubble transport equation is most lucidly demonstrated with a geometric argument given by Garabedian (1964, p. 18). The parametrically represented curve C in nine-dimensional space

$$\mathbf{R}(t) \equiv [t, x(t), y(t), z(t), v_x(t), v_y(t), v_z(t), l(t), \psi(t)], \quad -\infty < t < \infty,$$

obtained by integrating the characteristic equations (11) and (12), is called a 'characteristic curve'. Components of the initial point $\mathbf{R}(t_0)$ are called 'characteristics'. The family of characteristic curves

$$\{\mathbf{R}(t) \,|\, -\infty < t < \infty, \mathbf{R}(t_0) \in \mathscr{C}\},$$

parametrized by the set $\mathscr{C}$ of accessible characteristics, forms a hypersurface $\psi(t; \mathbf{r}_0, \mathbf{v}_0, l_0, t_0)$ in nine-dimensional space that satisfies the bubble transport equation.

The family of characteristic curves is essentially parametrized by the set of initial conditions $(\mathbf{r}_0, \mathbf{v}_0, l_0)$ because t_0 and $\psi_0(\mathbf{r}_0, \mathbf{v}_0, l_0)$, the initial distribution,

are usually fixed for a given problem. Since $\mathbf{a}$, ν and S are generally functions of $\mathbf{r}$, $\mathbf{v}$, l, and t, the solutions to (11) and (12) are not only functions of the parameter t, but they each depend upon all of these initial conditions. Thus

$$\mathbf{r} = \mathbf{r}(t; \mathbf{r}_0, \mathbf{v}_0, l_0, t_0) \equiv \mathbf{r}(t), \quad \mathbf{v} = \mathbf{v}(t; \mathbf{r}_0, \mathbf{v}_0, l_0, t_0) \equiv \mathbf{v}(t), \qquad (13a, b)$$

$$l = l(t; \mathbf{r}_0, \mathbf{v}_0, l_0, t_0) \equiv l(t), \quad \psi = \psi(t; \mathbf{r}_0, \mathbf{v}_0, l_0, t_0) \equiv \psi(t), \qquad (13c, d)$$

where the short notation on the right is used for brevity.

The characteristic equations (11) are simply the bubble dynamics equations. The bubble dynamics model used to construct $\mathbf{a}$ and ν (see §4), as well as the characteristics $(\mathbf{r}_0, \mathbf{v}_0, l_0)$, determines a 'trajectory' $(\mathbf{r}(t), \mathbf{v}(t), l(t))$ which is the projection of a characteristic curve from nine-dimensional space onto seven-dimensional space. Bubble trajectories in x, y, z space are likewise projections of characteristic curves.

Lagrangian and Eulerian representations

The parametric representation (13), obtained by integrating the characteristic equations simultaneously, describes the continuum from a Lagrangian frame of reference. In this description, bubbles are labelled by group according to their characteristics $(\mathbf{r}_0, \mathbf{v}_0, l_0)$. This moving frame follows a specific group, initially in $d^7\tau_0 = d^3r_0 d^3v_0 dl_0$ about $(\mathbf{r}_0, \mathbf{v}_0, l_0)$ at t_0, along a characteristic curve to $d^7\tau(t)$ about $(\mathbf{r}(t), \mathbf{v}(t), l(t))$ at t. At any time t, $\psi(t)\, d^7\tau(t)$ is the number of bubbles belonging to the group labelled (r_0, v_0, l_0) that are found in $d^7\tau(t)$ about

$$(\mathbf{r}(t), \mathbf{v}(t), l(t)).$$

On the other hand, the distribution $\psi(\mathbf{r}, \mathbf{v}, l, t)$, expressed with $\mathbf{r}$, $\mathbf{v}$, l and t as independent variables, more conveniently describes the continuum from an Eulerian viewpoint. The Eulerian frame is fixed, and attention is focused on the particular volume $d^7\tau$ about the point $(\mathbf{r}, \mathbf{v}, l)$. The instantaneous bubble density $\psi(\mathbf{r}, \mathbf{v}, l, t)\, d^7\tau$ is considered without regard to the characteristics of bubbles in the volume.

Formal solution

If the source $S(\mathbf{r}, \mathbf{v}, l, t)$ has the form (10), then (7) is analogous to the Boltzmann transport equation written for neutral particles (e.g. photons or neutrons) or charged particles (e.g. electrons) in a purely absorbing medium with distributed sources (Case & Zweifel 1967, pp. 31, 247). For example, neutrons will stream along their characteristic curves in x, y, z space, which are straight lines, until they are absorbed or until they escape from the medium. Similarly, the bubbles described by (7) stream along their characteristic curves in $\mathbf{r}$, $\mathbf{v}$, l space until they disappear ($l \to 0$) or until they escape from the medium. However, the characteristic curves defined by (11) are generally not straight lines in $\mathbf{r}$, $\mathbf{v}$, l space or any of its subspaces, such as x, y, z space.

With S given by (10), the formal solution to (7) is obtained by integrating (12):

$$\psi(t; \mathbf{r}_0, \mathbf{v}_0, l_0, t_0) = \psi(\mathbf{r}_0, \mathbf{v}_0, l_0, t_0) \exp\left[T_1(t, t_0) - T_2(t, t_0)\right] + \int_{t_0}^{t} S_1(\mathbf{r}(t'), \mathbf{v}(t')\, l(t'), t') \exp\left[T_1(t, t') - T_2(t, t')\right] dt', \qquad (14)$$

where $$T_1(t,t_0) = \int_{t_0}^{t} \Sigma_1(\mathbf{r}(t'), \mathbf{v}(t'), l(t'), t')\, dt'$$

and $$T_2(t,t_0) \equiv \int_{t_0}^{t} \Sigma_t(\mathbf{r}(t'), \mathbf{v}(t'), l(t'), t')\, dt'.$$

All integrals in this expression, and all similar integrals appearing elsewhere in this paper, are understood to be line integrals along the characteristic curve that passes through $(\mathbf{r}_0, \mathbf{v}_0, l_0)$ and $(\mathbf{r}, \mathbf{v}, l)$.

Equation (6) represents a differential equation satisfied by the Jacobian $\gamma(t,t')$ that transforms the volume element $d^7\tau$ from one point to another on the same characteristic curve. Integrating (6) yields

$$\gamma(t,t') = \exp[T_2(t,t')], \tag{15}$$

which can be used to rewrite (14):

$$\psi(\mathbf{r}, \mathbf{v}, l, t)\, d^7\tau = \exp[T_1(t,t_0)]\, \psi(\mathbf{r}_0, \mathbf{v}_0, l_0, t_0)\, d^7\tau_0 + \int_{t_0}^{t} \exp[T_1(t,t')]\, S_1(\mathbf{r}', \mathbf{v}', l', t')\, d^7\tau'\, dt', \tag{16}$$

where the abbreviations $\mathbf{r} = \mathbf{r}(t; \mathbf{r}_0, \mathbf{v}_0, l_0, t_0)$, $\mathbf{r}' = \mathbf{r}(t'; \mathbf{r}_0, \mathbf{v}_0, l_0, t_0)$, etc., have been used. From this expression it is apparent that the number of bubbles in $d^7\tau$ about $(\mathbf{r}, \mathbf{v}, l)$ at time t is the number originally in $d^7\tau_0$ about $(\mathbf{r}_0, \mathbf{v}_0, l_0)$ at t_0 plus (minus) those added (subtracted) by sources (sinks) along the characteristic curve between $(\mathbf{r}_0, \mathbf{v}_0, l_0)$ and $(\mathbf{r}, \mathbf{v}, l)$. If $\Sigma_1 \neq 0$ in (10) then the result is amplified (attenuated) by the factor $\exp[T_1]$ because of the creation (absorption) rate $\Sigma_1 \psi$ along the path. For $t = t_0 + dt$, equation (16) expanded in a Taylor series to $O(dt)$ yields equation (2), as it must.

Equations (7) and (16) are equivalent statements about the physical model outlined at the beginning of § 2. They formally represent relationships that exist between the bubble distribution, single-bubble dynamics and the bubble sources. As such, these equations can be used for calculations to investigate relationships among the three in real situations. For example, if any two are specified, properties of the third can be inferred, either directly or indirectly.

4. Single-bubble dynamics

Prior to using (16) for calculations, a bubble dynamics model must be specified so that equations (11) can be integrated to obtain the characteristic curves. In this section general expressions are derived for $\mathbf{a}$ and ν, and some known models of gas diffusion and drag are summarized for gas bubbles in liquids. For the purpose of discussion in this section and § 5, consider an inertial Cartesian co-ordinate system with the z axis vertically upward and the origin at the surface of the liquid. Let $\mathbf{v}$ be the bubble velocity and $\mathbf{V}(\mathbf{r}, t)$ be the transporting fluid's velocity relative to this frame of reference.

Acceleration

If a bubble of volume σ, containing fluid of density ρ, were completely entrained ($\mathbf{v} = \mathbf{V}$) by a fluid of density ρ_0, it would experience the same force $\rho_0 \sigma d\mathbf{V}/dt$ as would transporting fluid enclosed in the same volume. For $\rho \neq \rho_0$, partial

entrainment occurs, and the bubble maintains a relative velocity $\mathbf{u} \equiv \mathbf{v} - \mathbf{V}$, with respect to the transporting fluid. Hence, the bubble experiences a drag force $\mathbf{F}_D$, which will be discussed shortly in the context of gas bubbles in liquids.

As the bubble moves relative to the transporting fluid it 'drags' with it an amount of fluid having a volume equal to some fraction β of the bubble volume. By Newton's third law, this adhering mass provides a supplementary reaction term $-(\beta\sigma\rho_0 d\mathbf{u}/dt)$ that acts to increase the bubble's effective inertial mass. In addition, there is a net buoyant force $\sigma g(\rho_0 - \rho)\hat{\mathbf{k}}$, where $\hat{\mathbf{k}}$ is a vertically upward unit vector and g is the acceleration of gravity. Combining all of these forces in Newton's second law yields the following expression for acceleration:

$$\mathbf{a} = \mathbf{F}_D/(\sigma\rho_0(\beta + \rho/\rho_0)) + (1+\beta)(d\mathbf{V}/dt)/(\beta + \rho/\rho_0) + (1-\rho/\rho_0)g\hat{\mathbf{k}}/(\beta + \rho/\rho_0), \quad (17)$$

in which

$$d\mathbf{V}/dt = \partial\mathbf{V}/\partial t + (\mathbf{v}.\nabla_r)\mathbf{V}. \quad (18)$$

Drag on gas bubbles in a liquid

Because of its theoretical and practical importance, the motion of gas bubbles in liquids (e.g. air bubbles in water) has been actively studied (Levich 1962, §80). The regimes of bubble motion are classified according to the Reynolds number $Re = u\rho_0 l/\eta$, where η is the liquid's viscosity. Observations of different-size bubbles rising in various liquids indicate that small ($Re < 1$) and medium-size ($1 < Re < 700$) bubbles maintain a spherical shape, whereas large ($Re > 700$) bubbles deform to flattened ellipsoids and very large bubbles ($Re > 4500$) are unstable and tend to break up.

For small bubbles ($l \lesssim 100\,\mu$m in water) the drag is viscous in nature and is given by

$$\mathbf{F}_V = -\kappa\eta l\mathbf{u}, \quad (19)$$

with $\kappa = 4\pi$ for a perfectly clean bubble having a mobile two-fluid interface at its surface. However, most liquids such as water contain 'surface-active' materials that coat the bubble and destroy the mobility of this interface. In this case the relative velocity of the transporting fluid goes to zero at the bubble's surface, and the bubble behaves like a solid sphere, for which the drag is given by (19) with $\kappa = 6\pi$ (Levich 1962, §§70, 81).

The flow past medium-size bubbles ($100\,\mu\text{m} \lesssim l \lesssim 2000\,\mu$m in water) is separated, with the separation region occuping an area s_1 on the downstream portion of the bubble's surface. Up to the separation point the resistance that acts on the bubble is viscous in nature with a contribution to the total drag given by (19) with $\kappa = 12\pi$. Past the separation point and into the bubble's wake the flow is characterized by turbulent motion with a contribution to the total drag given by

$$\mathbf{F}_T = -0{\cdot}5K_f\rho_0 s_1 u\mathbf{u}, \quad (20)$$

where K_f is a drag coefficient with $0{\cdot}65 \lesssim K_f \lesssim 0{\cdot}55$ for $200 < Re < 1000$ (Levich 1962, §§80, 82).

In the absence of surface-active materials, s_1 is very small ($s_1 \sim l^2/R_e$ for $R_e \gg 1$), so flow past the bubble is essentially unseparated and the drag is given by

(19) with $\kappa = 12\pi$. On the other hand, when an area s_0 on the bubble is covered by a monolayer of surface-active material, the relative fluid velocity in this region is zero, and flow separation occurs there. In this case viscous drag (19) is accompanied by the form drag (20) with $s_1 = s_0$, and the latter dominates the former when

$$s_0/(4\pi l^2) \gtrsim 28(\eta/\rho_0)^2/(gl^3)$$

(Levich 1962, §82). For example, when $l = 500\,\mu$m, only 2 % of the bubble's surface need by covered by a monolayer of this material before the drag force becomes quadratic according to (20).

Radius change rate

For gas bubbles moving in a liquid such as water, radius changes are caused primarily by changes in pressure, due to changes in depth or surface tension, or by gas diffusion across the bubble surface. Spherical bubbles ($Re \lesssim 700$) that contain n moles of ideal gas at temperature T and pressure P are described by

$$\tfrac{4}{3}\pi l^3 = nRT/P, \tag{21}$$

where R is the gas constant. For isothermal processes, (21) is readily differentiated to yield

$$v = \frac{dl}{dt} = \frac{l}{3}\left(\frac{dn/dt}{n} - \frac{dP/dt}{P}\right). \tag{22}$$

Gas diffusion is included in the dn/dt term, while compression and surface tension are included in dP/dt. Assuming quasi-equilibrium, gas pressure is the sum of atmospheric pressure P_0, surface tension pressure $2\zeta/l$ and fluid weight $-\rho_0 gz$, where $-z \geqslant 0$ is the depth and ζ is the surface tension:

$$P = P_0 - \rho_0 gz + 2\zeta/l \tag{23}$$

and

$$dP/dt = -\rho_0 g v_z - (2\zeta/l^2)\, dl/dt. \tag{24}$$

Gas diffusion

As results of the next section will indicate, gas diffusion is one of the more important factors affecting the bubble distribution. It is a complex phenomenon depending upon many influences that include the type of gas in the bubble, the gas diffusivity D in the transporting liquid, the gas concentration C in liquid contacting the bubble's surface, the gas concentration C_∞ in liquid far away from the bubble, the presence of surface-active materials in the liquid and on the surface of the bubble, the flow field around the bubble and the bubble radius. To simplify the discussion here it will be assumed that gas inside the bubble is composed of one type of 'average' molecule having a single diffusivity D.

If the Péclet number is large, $Pe \equiv ul/D \gg 1$, the gas concentration gradient is confined to a thin boundary layer on the surface of the bubble, and diffusion between C and C_∞ occurs across a small distance $d \sim l/Pe^{\frac{1}{2}}$. Hence (Levich 1962, §§14, 72)

$$dn/dt = -Gl^2(C - C_\infty), \tag{25}$$

where the coefficient G is generally a function of l, u and D. For specific applications in which individual components of gas must be monitored, (25) will have to be generalized.

Typically $(\eta/\rho)/D \sim 10^3$, so there is a wide range of bubble radii for which the Péclet number is large ($Pe \gg 1$) but the Reynolds number is small ($Re < 1$). For that case (small bubbles),

$$G = 8[\tfrac{1}{6}\pi(Du/l)]^{\frac{1}{2}} \tag{26}$$

in the absence of surface-active material (Levich 1962, §§72, 91). In the presence of surface-active material, the flow field around a small bubble is like that around a solid sphere, and G becomes (Levich 1962, §14)

$$G = 8(D^2u/l^2)^{\frac{1}{3}}. \tag{27}$$

At moderate Reynolds numbers (medium-size bubbles) the flow is separated, but the region of separation s_1 is generally small. If gas diffusion across s_1 can be neglected, (25) represents the gas diffusion with G equal to (26) multiplied by $\sqrt{3}$ (Levich 1962, §91).

If liquid in contact with the bubble surface is assumed to always be saturated with gas at the pressure P (in atmospheres) prevailing inside the bubble, then $C = KP$, where K (kg m^{-3} atm^{-1}) is the absorption coefficient for the liquid–gas system. Defining the partial pressure $f \equiv C_\infty/K$ (in atm) of gas in the transporting fluid, (25) can be rewritten as

$$dn/dt = -GKl^2(P-f). \tag{28}$$

Under laboratory conditions, Wyman *et al.* (1952) measured the rate of solution and the change in composition of air bubbles in stirred sea water, as a function of depth. These experimental results follow very closely the law

$$dn/dt = -4\pi\delta l^2(P-f) \tag{29}$$

with $\delta \cong 4{\cdot}4 \times 10^{-5}$ moles m^{-2} s^{-1} atm^{-1}. Using (26) and (27) with published values of D and K for oxygen and nitrogen in water, estimates of GK for bubbles rising at terminal velocity are found to be comparable with $4\pi\delta$, but are generally larger. The presence of surface-active materials that retard gas diffusion and reduce the effective absorption coefficient across the bubble's surface may have contributed to the discrepancy (Fox & Herzfeld 1954).

5. Application to the upper ocean

The purpose of this section is to discuss briefly application of bubble transport theory to the description of gas bubble populations in the upper ocean. It is appropriate to begin with a summary of some observations concerning bubble sources S and fluid velocity fields $\mathbf{V}$ in the upper ocean. Then, to demonstrate an application of bubble transport theory, some sample calculations are performed and interpreted.

Bubble sources and fluid velocity fields

Physically one might consider bubble sources to be segregated into three categories according to depth: those on the ocean floor, those concentrated at the surface, and those distributed throughout the medium, principally near the surface. Mathematically these classifications are convenient for analysis since sources in the first two categories can be incorporated into (7) and (16) either as boundary conditions or as plane sources.

The first category includes sediment-initiated bubbles, which often contain organic gas (McCartney & Bary 1965). In the second category are bubbles generated at or very near the surface by wind and wave action, precipitation and captured aerosols (Blanchard & Woodcock 1957; Glotov *et al.* 1962; Medwin 1970; Monahan & Zietlow 1969). The third category includes bubbles initiated within the volume of the upper ocean by internal wave action, radiation and biological activity. Pressure changes and turbulence caused by wind-driven surface waves may nucleate small bubbles at distributed cavitation sites, while the vertical fluid velocity and turbulence created by breaking waves introduces larger bubbles below the surface.

When a wave breaks and air is rapidly mixed with water, the bubbles formed are entrained by a strong vertical velocity field; these bubbles have been observed as far as three wave heights below the surface (Kanwisher 1963). As the strong downward currents decay, the bubbles tend to rise under buoyancy with motion modified by the remaining fluid velocity field (see equation (17)).

Shonting (1968) has measured the autospectra of particle motions in the upper ocean and shown that the dominant peaks are associated with the frequencies of the surface waves. The spectral energy decays exponentially with depth in a way that attenuates high frequencies the most rapidly.

Example

Consider a one-dimensional steady-state ocean in which all velocities are vertical and in which all functions depend spatially on depth only. In this case the bubble transport equation reduces to

$$v\frac{\partial\phi}{\partial z}+a\frac{\partial\phi}{\partial v}+\nu\frac{\partial\phi}{\partial l}=-\Sigma_t\phi+S, \tag{30}$$

where $\phi(z,v,l)$ is the distribution function, $v_z=v$ is the vertical velocity, $a_z=a(z,v,l)$ is the vertical acceleration and $\Sigma_t=\partial a/\partial v+\partial\nu/\partial l$.

The characteristic equations for (30) can be written with $z\leqslant 0$ chosen as the independent parameter. This choice is equivalent to dividing equations (11) and (12) by (11*c*):

$$dv/dz=a(z,v,l)/v, \quad -\infty<v<\infty; \quad v(z_0)=v_0; \tag{31}$$

$$dl/dz=\nu(z,v,l)/v, \quad 0\leqslant l<\infty; \quad l(z_0)=l_0; \tag{32}$$

$$d\phi/dz+(\Sigma_t/v)\,\phi=S(z,v,l)/v, \quad 0\leqslant\phi<\infty; \quad \phi(z_0)=\phi_0(v_0,l_0). \tag{33}$$

Simultaneous integration of (31) and (32) yields the family of characteristic curves

$$\{z, v(z; z_0, v_0, l_0), l(z; z_0, v_0, l_0); z \leqslant 0\}, \tag{34}$$

and bubble trajectories in x, y, z space are vertical straight lines.

A formal solution analogous to (14) is readily obtained by integrating (33) along characteristic curves (34). The form analogous to (16),

$$v\phi(z, v, l)\, dv\, dl = v_0 \phi(z_0, v_0, l_0)\, dv_0 dl_0 + \int_{z_0}^{z} S(z', v', l')\, dz'\, dv'\, dl', \tag{35}$$

is derived using the Jacobian,

$$\frac{\partial(v, l)}{\partial(v', l')} = \frac{v'}{v} \exp\left[\int_{z'}^{z} \frac{\Sigma_t(z'', v'', l'')}{v''} dz''\right]. \tag{36}$$

Physical insight into (35) can be gained by reflecting on a situation where there are no distributed sources, $S = 0$, so that

$$\phi(z;\, z_0, v_0, l_0)\, dv\, dl = (v_0/v)\, \phi(z_0, v_0, l_0)\, dv_0 dl_0.$$

If there is no fluid velocity, bubbles rise under buoyancy at a terminal velocity and may shrink and slow down or expand and speed up (LeBlond 1969*a*, *b*). Those belonging to the Lagrangian group (z_0, v_0, l_0) whose velocities increase with z have a spatial density that decreases as z increases because the bubbles at $z + dz$ are running away from those at z. On the other hand, those whose velocities decrease as z increases have a density increasing with z since the bubbles at z are piling up on those at $z + dz$.

Characteristic curves. A first step towards using (35) to calculate the bubble distribution is the specification of $a(z, v, l)$ and $\nu(z, v, l)$ and the computation of characteristic curves (34). A useful expression for the radius change rate is obtained by substituting (21), (23), (24) and (28) into (22) and solving for dl/dt. Then (32) becomes

$$dl/dz = \nu/v = \{\tfrac{1}{3}l - (GK/4\pi)(RT)[D(1-f) - z + (\Gamma/l)]/v\}/[D - z + (\tfrac{2}{3})(\Gamma/l)], \tag{37}$$

where $-z$ is the depth, $f(z)$ is the partial pressure (in atmospheres) of gas in the water, $D \equiv P_0/\rho_0 g \cong 10$ m is the depth of sea water equivalent to one atmosphere, and $\Gamma \equiv 2\zeta/\rho_0 g \cong 1{\cdot}47 \times 10^{-5}\,\mathrm{m}^2$ is a surface tension coefficient in water. Note that the Γ/l terms are negligible unless the bubbles are very small ($l \lesssim 30\ \mu$m).

The acceleration is given by (17) with the drag force given by (19) or (20). If the fluid velocity is negligible ($\mathbf{V} \cong 0$), the bubbles rise very nearly at their terminal velocity v_T. This is seen in figure 1, which was obtained by simultaneously integrating (31) and (37) numerically† for bubbles of various initial radii l_0, starting from rest at $z_0 = -20$ m. Small bubbles ($l < 100\,\mu$m), and medium-size bubbles ($100\,\mu\mathrm{m} < l < 2000\,\mu\mathrm{m}$) with viscous drag dominant, rise at a terminal velocity v_{T1} given approximately by equating (19) to the buoyancy force:

$$v_{T1} = (g/(\kappa'\alpha))\, l^2, \tag{38}$$

where $\kappa' = 1$ and $\kappa' = 2$, respectively, and where

$$\alpha \equiv \tfrac{9}{2}\eta/\rho_0 \cong 4{\cdot}37 \times 10^{-6}\,\mathrm{m}^2/\mathrm{s}$$

† All numerical integrations alluded to in this section were carried out using Gaussian quadrature or an optimal fourth-rank Runge–Kutta technique (Ceschino & Kuntzmann 1966, p. 67).

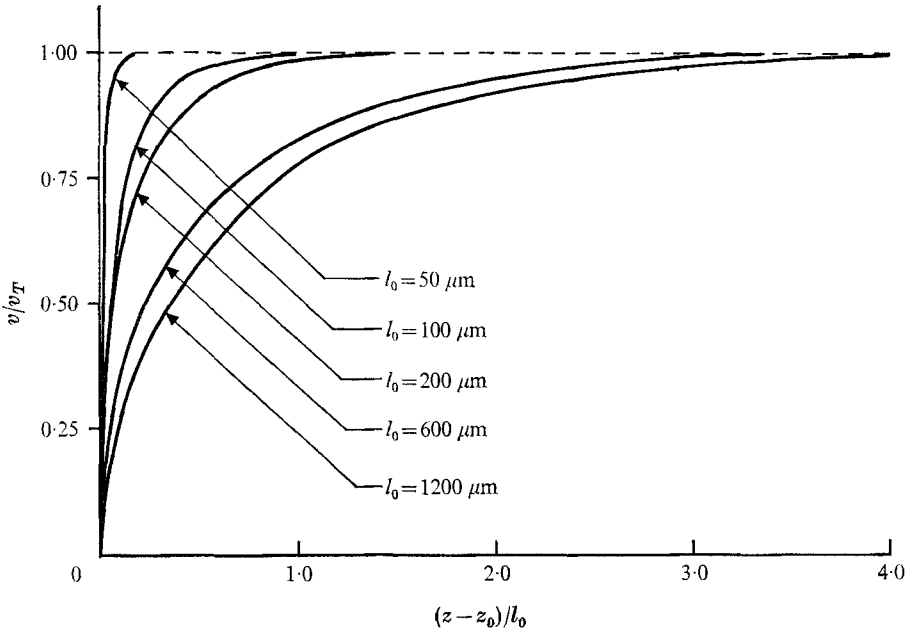

FIGURE 1. The velocity v of bubbles starting at rest and rising from an initial depth $z_0 = -20$ m. The initial radius is l_0 (in microns), the terminal velocity is v_T, and $z - z_0$ is the height above the release point.

in water. When medium-size bubbles have a sufficient fraction of their surface,

$$\epsilon \equiv s_0/(4\pi l^2),$$

covered by a monolayer of surface-active material, turbulent drag dominates viscous drag because flow separation occurs at the boundary of s_0. They rise at a terminal velocity v_{T2} given approximately by equating (20) to the buoyancy force:

$$v_{T2} = (g/\xi)^{\frac{1}{2}} l^{\frac{1}{2}}, \tag{39}$$

where

$$\xi \equiv \tfrac{3}{2} K_f \epsilon \cong 0{\cdot}9\epsilon.$$

In general the terminal velocity of a rising bubble is not given simply by (38) or (39) during its entire lifetime. Many bubbles shrink or expand as they rise (LeBlond 1969*a*, *b*) and thereby transition from the regime of predominantly turbulent drag to the regime of predominantly viscous drag, or vice versa. The treatment of separated flow in Levich (1962, §82) suggests that the sum of (19) and (20) should be a useful model for the drag on medium-size bubbles in the transition region. Using this model in (17), equation (31) can be written as

$$dv/dz = -[(\xi/\beta)/l]\,[(v - v_-)\,(v + v_+)/v], \tag{40}$$

where

$$v_\pm \equiv v_{T2}[\pm 1 + (1 + 4Q^2)^{\frac{1}{2}}]/2Q \tag{41}$$

with $Q \equiv v_{T1}/v_{T2} = (l/\tilde{l})^{\frac{3}{2}}$ and $\tilde{l} \equiv [(\kappa'\alpha)^2/(g\xi)]^{\frac{1}{3}}$. This approach appears to have some merit since (41) for v_- yields values close to the empirical curve produced by Datta, Napier & Newitt (1950), who averaged the results of several observers,

and since the model shows the proper limiting behaviour in the viscous ($l < \tilde{l}$) as well as the turbulent ($l > \tilde{l}$) regimes.

Computation of characteristic curves (34) in a quiescent fluid ($\mathbf{V} = 0$) is simplified because the bubble velocity is always very nearly the terminal velocity, $v \approx v_T(z; z_0, l_0)$, and is essentially independent of v_0. Either (38), (39), (41) or empirical values for v_T can be used in (37) to obtain $l(z; z_0, l_0)$. If (38) or (39) is used and surface tension is neglected, approximate analytical expressions can be developed. If gas diffusion as well as surface tension is neglected, then the extremely simple approximate analytical result

$$l = l_G(z; z_0, l_0) = [(D - z_0)/(D - z)]^{\frac{1}{3}} l_0 \tag{42}$$

is obtained.

Bubble distribution. For bubbles rising in a quiescent fluid,

$$\phi(z, v, l) = \delta(v - v_T)\, \Phi(z, l) \tag{43}$$

should be a good approximation, where v_T is given either empirically or by (38), (39) or (41), and where

$$\Phi(z, l) \equiv \int_{-\infty}^{\infty} \phi(z, v, l)\, dv$$

is the 'radius density', the number of bubbles per unit volume per unit radius. Using (43) in (35) and integrating over v yields

$$\Phi(z, l) = \frac{v_{T0}}{v_T} \Phi(z_0, l_0) \frac{\partial l_0}{\partial l} + \frac{1}{v_T} \int_{z_0}^{z} s(z', l') \frac{\partial l'}{\partial l} dz' \tag{44}$$

with

$$s(z', l') \equiv \int_{-\infty}^{\infty} S(z', v', l')\, dv',$$

where $dl_0 = (\partial l_0/\partial l)\, dl$ and $dl' = (\partial l'/\partial l)\, dl$ have been used.

For most applications the radius density provides adequate information. To calculate this function for a given z and l, one needs $\partial l'/\partial l$, l' and $s(z', l')$ at points on the characteristic curve that passes through (z, l) so that the integral in (44) can be evaluated. Taking the partial derivative of (37) with respect to l' and setting $v = v_T$ results in a differential equation for $\partial l/\partial l'$ that can be integrated to obtain

$$\partial l/\partial l' = \exp\left[\int_{z'}^{z} F(z''; z_0, l_0)\, dz''\right], \tag{45}$$

where

$$\begin{aligned} F(z; z_0, l_0) &= \{(2\Gamma/l^2)\,[l - (3\delta RT/v_T)\,(D(1-f) - z + \Gamma/l)]\,[3(D-z) + 2\Gamma/l]^{-1} \\ &\quad + [1 + (3\delta RT/v_T)\,[\Gamma/l^2 + (D(1-f) - z + \Gamma/l)\,(\partial v_T/\partial l)/v_T]]\}\,[3(D-z) + 2\Gamma/l]^{-1}, \end{aligned} \tag{46}$$

in which $GK/4\pi = \text{constant} \equiv \delta$ (Wyman *et al.* 1952) has been used. When the approximation (41) is used,

$$\partial v_T/\partial l = (3v_{T1}/l)\,[1 + 4Q^2]^{-\frac{1}{2}} - v_-/l. \tag{47}$$

In the following discussion of sample calculations, $\Phi(z, l)$ will designate the radius density when (41) and (45)–(47) are used in (37) and (44). $\Phi_G(z, l)$ will

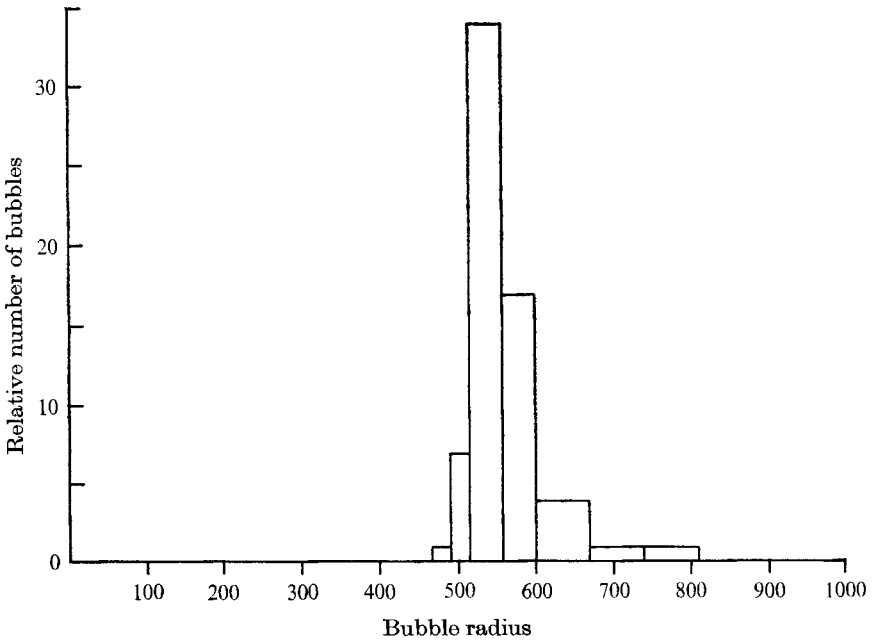

FIGURE 2. The distribution $\Phi(z_0, l_0)$ in relative units, of bubbles rising off the bottom of Saanich Inlet, B.C. (McCartney & Bary 1965), where $z_0 = -197$ and the bubble radius l_0 is in microns.

designate the approximate radius density when (42) is used in (44). For the sake of brevity, semi-analytical results obtained using the approximations (38) and (39) are not included.

Sample calculations. As a first example, consider the situation investigated by McCartney & Bary (1965), who acoustically measured rather large gas bubbles ascending from the bottom of Saanich Inlet, B.C., and inferred the bottom source represented in figure 2 from the ascent velocities. If we model that ocean as one-dimensional and quiescent, then (44) can be used to infer the radius density throughout the volume. Since volume sources produce mainly smaller bubbles that the measurements of McCartney & Bary do not include, only the plane source $\Phi(z_0, l_0)$ (figure 2) at $z_0 = -197$ m is considered in this sample calculation, and (44) reduces to

$$\Phi(z, l) = (v_{T0}/v_T)\,\Phi(z_0, l_0)\,(\partial l_0/\partial l). \tag{48}$$

Using $f = 1$, the radius density Φ and the approximation Φ_G were computed at various depths between $z = -197$ m and $z = 0$. $\Phi(z, l)$ (solid line) and $\Phi_G(z, l)$ (dashed line) are plotted in figures 3 and 4 at the depths $z = -147$ m, $z = -47$ m and $z = 0$. Although actual calculations do not yield precisely rectangular distributions for $z \neq z_0$, Φ and Φ_G are drawn as perfect histograms because the error introduced is negligible.

While Φ_G neglects gas diffusion and surface tension, Φ includes these effects. For the gas diffusion model used, all bubble radii for which $\Phi(z_0, l_0)$ is non-zero are sufficiently small such that these bubbles will shrink monotonically as they

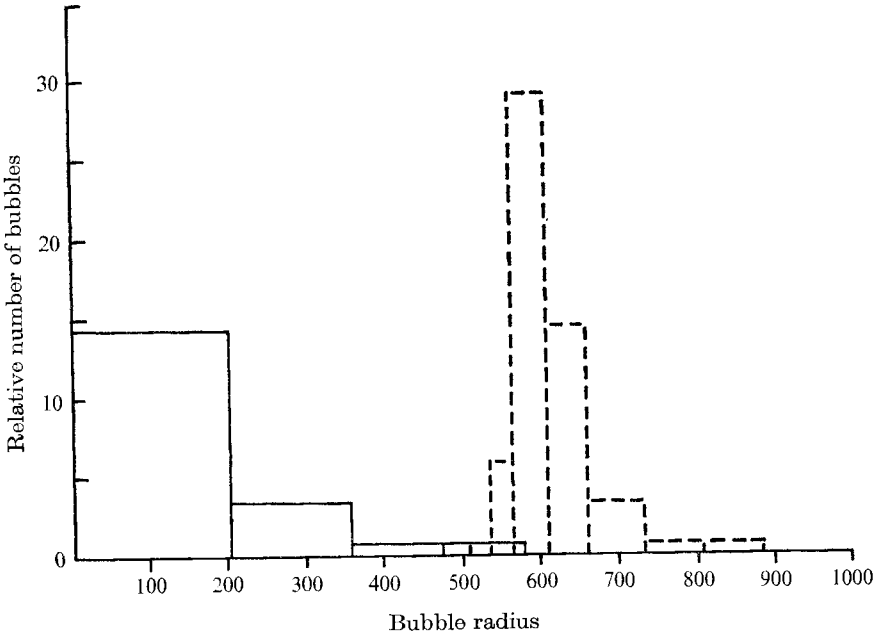

FIGURE 3. The distributions $\Phi(z, l)$ (solid line) and $\Phi_G(z, l)$ (dashed line) in relative units at a depth $z = -147$ m, where the bubble radius l is in microns. Φ_G neglects gas diffusion while Φ assumes a uniform partial pressure of one atmosphere, $f = 1$, and $RTGK/4\pi = 10^{-6}$ m/s (Wyman *et al.* 1952).

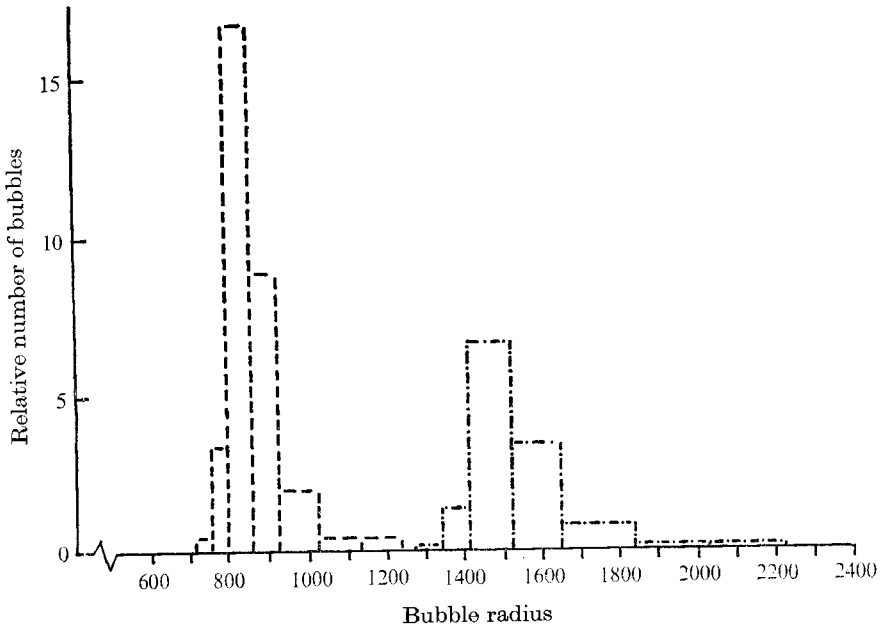

FIGURE 4. The distribution $\Phi_G(z, l)$, in relative units, *vs.* radius l, in microns, for $z = -47$ m (dashed line) and $z = 0$ (broken line).

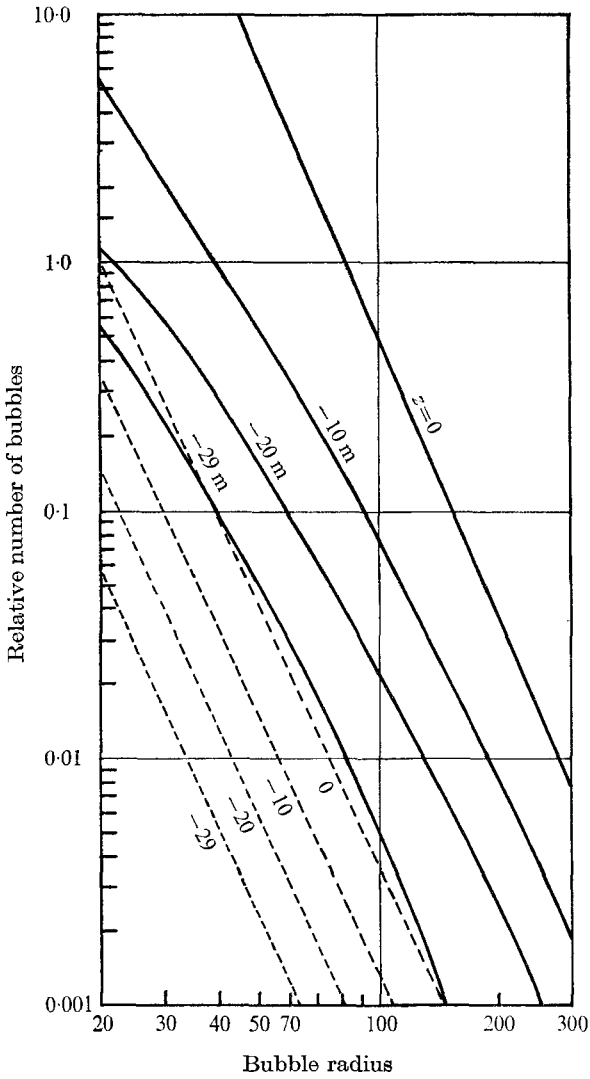

FIGURE 5. The distribution $\Phi(z, l)$ (solid lines), *in relative units, vs. radius* l, *in microns*, for various depths, in metres, from a distributed source $s(z, l)$ (– – – –, equations (49) and (50)). The same gas diffusion model as was used to calculate Φ in figure 3 is used in this example.

rise and will disappear before reaching the surface (Le Blond 1969*a*, *b*). The distribution Φ is seen to shift toward smaller radii as depth decreases, until even the largest bubbles have disappeared by the time $z \sim -90$ m, so only Φ_G is shown in figure 4. In the model used to calculate Φ_G, the bubbles necessarily expand as they rise, and the distribution shifts monotonically to larger radii.

The bubble density is simply the area under the histogram. As z increases from -197 m the density of $\Phi(z, l)$ initially increases since flux is conserved and the bubbles are slowing down and piling up. However, nearer the surface, most smaller bubbles have succumbed to gas diffusion and the density starts to de-

crease toward zero. For $\Phi_G(z,l)$ the density is seen to decrease as z increases since the bubbles are accelerating and becoming spread out.

Interestingly enough, the experimental results of McCartney & Bary (1965) indicate that bubbles from the bottom of Saanich Inlet expand as they rise according to the distribution Φ_G, which ignores gas diffusion. Thus, it appears the diffusion is somehow inhibited across the surfaces of these bubbles, which are composed of 'gas released from the highly organic, anaerobic sediment of the bottom', possibly methane. Either the water was saturated with respect to the gas(es) in the bubbles, or these bubbles were coated with an active material that severely impeded gas diffusion. It is significant to note that Φ is calculated using $GK/4\pi = \delta$ (equation (29)), which is based upon experiments with relatively clean *air* bubbles (Wyman *et al.* 1952), and that $f = 1$ at all depths is not physically realistic. However, certain qualitative conclusions, based on a comparison of Φ and Φ_G to the observed distribution, are still valid, For example, gas diffusion appears to be negligible in this situation; and gas diffusion as from clean bubbles would profoundly affect the distribution. The latter observation emphasizes the fact that calculated results are strongly dependent on certain aspects of the bubble dynamics and ocean models used.

As the basis for a second sample calculation, consider the supposition that the observed bubble distribution indicates the functional dependence of the volume source. To test this idea, consider a hypothetical volume source suggested by the measurements of Shulkin (1968) and Medwin (1970):

$$s(z,l) = e^{z/h}L(l), \tag{49}$$

where

$$L(l) = \begin{cases} (l/l')^{-3\cdot5} & \text{for} \quad l \geqslant l'. \\ 0 & \text{for} \quad 0 \leqslant l < l' \end{cases} \tag{50}$$

with $h = 10\,\text{m}$ and $l' = 20\,\mu\text{m}$. Physically, a source decaying exponentially with depth might arise from photosynthesis, light-sensitive bacteria, wave action, etc. Medwin (1970) has observed an exponential behaviour for small bubbles ($l \lesssim 60\,\mu\text{m}$), and both Medwin (1970) and Shulkin (1968) have observed that the near-surface bubble density appears to fall off like some power of the bubble radius. The radius spectrum $L(l) \sim l^{-3\cdot5}$ is chosen as an example.

Under the assumption that the source is zero below $z = -30\,\text{m}$ and that $f = 1$, figure 5 presents log–log plots of $\Phi(z,l)$ (solid line) and $s(z,l)$ (dashed line) *vs.* radius for four depths, $z = -29\,\text{m}$, $-20\,\text{m}$, $-10\,\text{m}$ and 0. A comparison of Φ and s indicates that the distribution follows approximately the functional form of the source for $l \lesssim 100\,\mu\text{m}$:

$$\Phi(z,l) \sim e^{z/h'}l^{-3\cdot5}, \tag{51}$$

with $h' \cong 6{\cdot}5\,\text{m}$. The distribution at $z = -29\,\text{m}$ does not fit this pattern because it is too near the region assumed to be devoid of bubbles.

For $l \gtrsim 100\,\mu\text{m}$ the functional form of Φ is more complicated and does not necessarily follow (51). Except at the surface, the curves are all concave down, which indicates a deficiency of small bubbles. Gas diffusion and surface tension cause small bubbles to disappear much more rapidly than large bubbles. While the small bubbles observed at a given depth originate primarily from local

sources, many of the larger bubbles originate at sources distributed well below that depth. However, for the model used, gas diffusion decreases rapidly with depth, so there is less discrimination against the small bubbles in the near-surface region. From figure 5,

$$\Phi(0, l) \sim l^{-3\cdot75}. \tag{52}$$

These results indicate that if gas diffusion is significant the small-bubble sources will probably fall off at a higher power of l than the observed distribution, but the larger-bubble sources may have roughly the same l dependence as the observed distribution. Furthermore, the depth dependence of the bubble sources is likely to be functionally similar to that of the bubble population. Of course these qualitative relationships between bubble population and bubble sources are not likely to be applicable unless the model is valid. For example, any of the following can have a profound influence on the bubble distribution and its relationship to the source: a significant fluid velocity $\mathbf{V} \neq 0$, a partial pressure $f(z)$ that varies with depth, or surface-active materials that impede gas diffusion (e.g. lower K in equation (28)).

6. Conclusions

The main purpose of this paper has been to develop the general framework of bubble transport theory and then to demonstrate its application. The bubble transport equation and its solution relate the ensemble-average behaviour of a bubble population to the dynamics of a single bubble and to properties of the transporting fluid. Among the most important aspects of gas bubble dynamics in liquids are bubble gas diffusion and drag, which depend upon many different physical parameters. For the upper ocean, information concerning these parameters, as well as information about bubble sources and fluid velocity fields, is usually incomplete. In this application, bubble transport theory cannot be used to predict bubble distributions or to explain all of their properties. Instead its primary utility is as an analytical tool for investigating relationships among the various complex factors that affect the distribution and for refining models of the upper ocean. Future work will involve analyses of increasingly complex ocean models with the objective of understanding more about observed bubble populations.

I would like to thank Professor Herman Medwin, who was an invaluable consultant, and the referees who provided many useful suggestions. Most of the numerical results in §5 are based upon calculations performed by Frank H. Heistand, Lt, U.S.N., and Thomas C. Vajda, Lt, U.S.N. This research was partially supported by the Naval Ship Systems Command, Code (PMS 302).

REFERENCES

Blanchard, D. C. & Woodcock, A. H. 1957 *Tellus*, **9**, 145.

Case, K. M. & Zweifel, P. F. 1967 *Linear Transport Theory*. Addison-Wesley.

Ceschino, F. & Kuntzman, J. 1966 *Numerical Solution of Initial Value Problems*. Prentice-Hall.

Chapman, S. & Cowling, T. G. 1964 *The Mathematical Theory of Non-Uniform Gases*, Cambridge University Press.

Datta, R. L., Napier, D. H. & Newitt, D. M. 1950 *Trans. Inst. Chem. Engrs, Lond.* **23**, 14.

Fox, F. E. & Herzfeld, K. F. 1954 *J. Acoust. Soc.* **26**, 984.

Garabedian, P. R. 1964 *Partial Differential Equations*. Wiley.

Glotov, V. P., Kolobaev, P. A. & Neuimin, G. G. 1962 *Sov. Phys. Acoust.* **7**, 341.

Kanwisher, J. 1963 *Deep-Sea Res.* **10**, 195.

LeBlond, P. H. 1969*a* *J. Fluid Mech.* **35**, 711.

LeBlond, P. H. 1969*b* *J. Fluid Mech.* **38**, 861.

Levich, V. G. 1962 *Physicochemical Hydrodynamics*. Prentice-Hall.

McCartney, B. S. & Bary, B. McK. 1965 *Deep-Sea Res.* **12**, 285.

Medwin, H. 1970 *J. Geophys. Res.* **75**, 599.

Monahan, E. C. & Zeitlow, C. R. 1969 *J. Geophys. Res.* **74**, 6961.

Shonting, D. H. 1968 *J. Mar. Res.* **26**, 43.

Shulkin, M. 1968 *J. Acoust. Soc. Am.* **44**, 1152.

Shulkin, M. 1969 *J. Acoust. Soc. Am.* **45**, 1054.

Sutcliff, W. H., Baylor, E. R. & Menzel, D. W. 1963 *Deep-Sea Res.* **10**, 233.

Wyman, J., Scholander, P. F., Edwards, G. A. & Irving, L. 1952 *J. Mar. Res.* **11**, 47.